[1]

# QUADRILATERAL MESHES WITH NO SMALL ANGLES

CHRISTOPHER J. BISHOP

Abstract. We show that any planar $n$-gon can be meshed by $O(n)$ quadrilaterals with all new angles bounded between $45 - \epsilon$ and $135 + \epsilon$.

[1]This is a preliminary version. Please do not distribute copies without author's consent. I have revised the meshing near the verticies to improve the angle bounds to be between 60 and 120, but have not yet modified the "merging" part of the argument to reflect this.

1991 *Mathematics Subject Classification.* Primary: 30C62 Secondary:

*Key words and phrases.* Quadrilateral meshes, Riemann mapping, thick/thin decomposition, linear time.

The author is partially supported by NSF Grant DMS 04-05578.

## 1. Introduction

In this note we answer a question of Bern and Eppstein by proving:

**Theorem 1.1.** *For any $\epsilon > 0$, a simply connected polygonal domain $\Omega$ with $n$ sides has a quadrilateral mesh with $O(n)$ pieces so that all new angles are between $45 - \epsilon$ and $135 + \epsilon$. The mesh can be constructed in time $O(n)$.*

Obviously we have to limit the lower bound to new angles, since existing angles of polygon can only be made smaller. The constant in $O(n)$ depends on $\epsilon$, and blows up as $\epsilon \to 0$, although this may only be an artifact of the proof. Although there is linear time algorithm for finding the mesh, it is perhaps best to think of this as an existence proof, since the constant in the $O(n)$ is likely to be very large.

This result was motived by results by Bern and Eppstein in [2] which give $O(n)$ size quadrilateral meshes with various special geometries (kites, opposite right angles, no big angles). In particular, they give a $O(n \log n)$ algorithm for finding a $O(n)$ complexity quadrilateral mesh with no angles bigger than $120°$ and show that 120 is optimal. Thus the novel aspect of Theorem 1.1 is the lower bound (and possibly the asymptotic linear time). Note that for triangulations, no such lower bound is possible, since even a $1 \times n$ rectangle will need $\Omega(n)$ triangles if we require a lower bound on the angles.

The main idea in the proof of Theorem 1.1 is to decompose $\Omega$ into $O(n)$ "thick" and "thin" parts. The thin parts have simple shapes and we can construct an explicit mesh in each of them. The thick parts are more complicated, but the Riemann map from the upper half-plane to $\Omega$ is well behaved there and we can transfer a mesh from $\mathbb{H}$ to the thick parts of $\Omega$ with small distortion. Finally, we have have to merge the meshes corresponding to the thick and thin parts (which is easy).

The thin parts of $\Omega$ correspond to pairs of sides of $\Omega$ which have small extremal distance in $\Omega$. This always happens for adjacent edges, so there is a thin part associated to each vertex and we call these the parabolic thin parts (this is an analogy with the theory of Riemann surfaces, see Section 3). It can also happen for a pair of non-adjacent edges, and such thin parts we call hyperbolic. More precisely, we say $\Omega$ has an hyperbolic $\epsilon$-thin part if there is a pair of non-adjacent sides whose extremal distance in $\Omega$ is $\leq \epsilon$ (adjacent edges are extremal distance 0 apart). A polygon with no hyperbolic $\epsilon$-thin parts will be called "$\epsilon$-thick".

It will be clear from our construction that only the hyperbolic thin parts require long narrow pieces in the mesh. We will say that a quadrilateral has "bounded geometry" if all its angles are in a compact subinterval of $(0, 180)$ and if all four sides are of comparable length. If $\Omega$ is $\epsilon$-thick, then our proof will show it can be meshed with $O(n/\epsilon)$ quadrilaterals of bounded geometry. Moreover, if $\{H_k\}_{k=1}^N$ is an enumeration of the hyperbolic thin parts and if $H_k$ is $\epsilon_k$-thin, then $\Omega$ can be meshed with $O(n + \sum_{k=1}^N \epsilon_k^{-1})$ quadrilaterals with bounded geometry, and this is sharp.

Because of the lower bound in Theorem 1.1, small angles on the polygon cannot be further subdivided, since this would create new small angles. Indeed, no vertex on $\partial\Omega$ with angle $\leq 120°$ will be subdivided by the mesh; Vertices with angle between $120°$ and $240°$ will be vertices of two quadrilaterals (each with exactly half the angle measure), and angles between $240°$ and $360°$ will be divided into four equal angles.

The rest of the paper in organized as follows:

**Section 2:** Given a finite set of reals, we define the associated sawtooth domain, define thick and thin parts of it and cover the thick part by a quadrilateral mesh.

**Section 3:** We describe the decomposition of a polygon into thick and thin parts. This section is for motivation and is not required for the proof of Theorem 1.1.

**Section 4:** We review some basic facts about conformal maps and show how to transfer the mesh of the thick part of the sawtooth domain to the thick part of the the polygon.

**Section 5:** We show how to mesh the hyperbolic thin parts by explicit construction.

**Section 6:** We show how to mesh the parabolic thin parts by explicit constructions.

**Section 7:** We discuss some questions for further investigation.

I would like to thank Marshall Bern for asking me the question which lead to Theorem 1.1 and pointing out [2] to me.

## 2. Covering the thick part of a sawtooth domain

In this section we will take a set $S \subset \mathbb{R}$ witwithh $n$ elements, define a "sawtooth" domain in the upper half-plane associated to this set, divide this domain into $O(n)$

"thick" and "thin" parts and cover the thick parts with $O(n)$ squares with the property that they can each be expanded by a fixed amount without hitting $S$. Later in the paper, the set $S$ will be taken to be the preimages of the vertices of a $n$-gon under a conformal map from the half-plane to the polygon, but will make no use of this yet.

In the upper half plane model, $\mathbb{H}$, the hyperbolic metric is given by

$$|d\rho| = \frac{|dz|}{\operatorname{dist}(z, \partial\mathbb{R})}.$$

Given an interval $I \subset \mathbb{R}$, the corresponding Carleson square is the region in the upper half-plane of the form $\{z = x + iy : x \in I, 0 < y < |I|\}$. The "top" of $Q$ is $T(Q) = \{z \in Q : y > |I|/3\}$. (It is more standard to take $y > |I|/2$, but the "3" will be more convenient for our purposes.) $T(Q)$ will be called a Whitney box, and its Euclidean diameter is comparable to its Euclidean distance from $\mathbb{R}$, and hence it is approximately unit size in the hyperbolic metric. A ternary Whitney box or Carleson square will be one corresponding to a base interval of the form $[j3^{-k}, (j+1)3^{-k}]$. Such boxes obviously form an infinite tree, with each box adjacent to three "children" and one "parent".

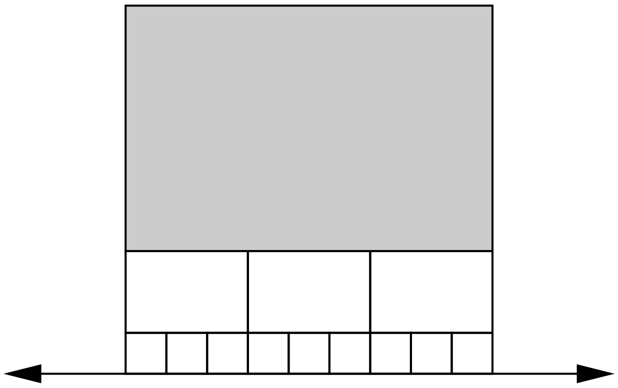

FIGURE 1. A decomposition of a Carleson square into ternary Whitney boxes.

Given a set of $n$ points $S \subset \mathbb{R}$, we define the associated "sawtooth" domain $W$ to be the union of all cones $C_s = \{x + iy : |x - s| < y\}$ for $s \in S$. See Figure 2. Let $\mathcal{C}$ denote the collection of all Whitney boxes which hit $W$. This is an infinite collection and we want to reduce it to a collection of $O(n)$ boxes which cover the most "interesting" parts of $W$.

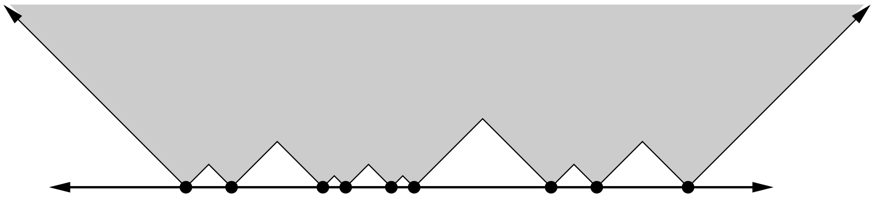

FIGURE 2. The sawtooth domain associated to the set $S$.

The medial axis of a planar domain $\Omega$ is the set of centers of all open disks $D \subset \Omega$ such that $\partial D \cap \partial\Omega$ has at least two points. $W$ is a polygon with at most $2n$ sides and we can compute the medial axis of $W$ in time $O(n)$ by a result of Chin, Snoeyink and Wang [5]. The full strength of their result is not needed; since $W$ is a monotone histogram, the medial axis can be computed (as described in [5]) using a modification of the method for convex polygons given in [**?**].

The medial axis of a polygon is a tree with three types of edges: point-point bisectors, point-edge bisectors and edge-edge bisectors. An edge-edge bisector for $W$ must be a vertical line segment. Enumerate all the edge-edge bisectors (there are at most $O(n)$ such edges) and compute their hyperbolic length (which is just $\log y/x$ if their endpoints are at heights $x < y$ above $\mathbb{R}$.

Fix some $A > 1$ and consider all the edge-edge bisectors that have hyperbolic length $\geq 2A$. Such an edge may either have finite or infinite hyperbolic length and we refer to these cases as hyperbolic and parabolic, respectively (we shall see later these names come from an analogy with hyperbolic surfaces). For any such edge $e$, let $e' \subset e$ be the points which are more than hyperbolic distance $A$ from either endpoint of $e$. This is called the central part of $e$ and $e'' = e \setminus e'$ is called the outer part. For each edge $e$, the outer part $e''$ consists of either one or two segments (in the parabolic and hyperbolic cases respectively), each of hyperbolic length $= A$. Each central part $e'$ has one or two endpoints in $W$ (in the same cases). By shortening the central part by at most hyperbolic length $\log 3$ at either end, we may also assume that the ends occur at heights above $\mathbb{R}$ which are powers of 3 (i.e., the endpoints lie on the boundary of a ternary Whitney box). For each such endpoint $x$, draw a horizontal line segment in $W$ through $x$ with its endpoints on $\partial W$. This segment divides $W$ into exactly two components. Let $\mathcal{H}$ denote the collection of all such horizontal segments (there are $O(n)$ of then since there are $O(n)$ edges of the medial axis of $W$). This collection of segments divides $W$ into a finite number of components. The components which contain a central segment of a edge-edge bisector will be called the thin parts of $W$ (parabolic or hyperbolic depending on the type of edge it contains) and the remaining components are called the thick parts of $W$ and their union will be denoted $W^{\text{thick}}$. Note that hyperbolic thin parts are Euclidean trapezoids and parabolic thin parts are Euclidean triangles one vertex on $\mathbb{R}$ at the corresponding point of $S$ (except for one unbounded parabolic thin part which is a truncated cone; we can think of this as a triangle with one vertex at $\infty$).

Let $\mathcal{C}_1 \subset \mathcal{C}$ be the set of Whitney boxes which hit $W_{\text{thick}}$. According to Lemma 18 of [4] at most $O(nA)$ binary Whitney boxes hit the medial axis outside the central segments and these boxes can be found in linear time. The same is true for ternary Whitney boxes, as can be seen by repeating the proof or noting that each binary Whitney box intersects only $O(1)$ ternary Whitney boxes. See Figure 3. Let $W_1$ be the union of the Whitney boxes in $\mathcal{C}_1$.

Next we modify our collection $\mathcal{C}_1$. First, add all the Carleson squares whose top edge meets a box in $\mathcal{C}_1$, but whose interior is disjoint from $W_1$. These squares "fill in" the gap between $W_1$ and $\mathbb{R}$ except for $O(n)$ regions, one for each central segment $e'$ of the medial axis of $W$. Next, subdivide each Whitney box into 6 Euclidean squares of equal size. Finally, fix some integer $k > 1$ and divide every square in the collection into $M^2 = 3^{2(k-1)}$ equal, disjoint subsquares. Call the resulting collection of $O(n)$ squares $\mathcal{C}_2$ and let the union of these squares be denoted $W_2$.

Then $\mathbb{H} \setminus W_2$ has $O(n)$ components, one for each thin part of $W$. We want to add some more squares to our collection so that the boundaries of the complementary components have a special shape: the edge of a $1 \times 2$ rectangle with a long edge on the real axis (equivalently, the boundary of the union of two adjacent Carleson squares of the same size).

To accomplish this, first consider segements in $\mathcal{H}$ which are bottom edges of thin parts (this happens at the bottom of every hyperbolic thin part and at the bottom of the single unbounded parabolic thin part). Let $S$ be such a segment, associated to medial axis edge $e$ and let $x \in \mathbb{R}$ be the vertical projection of this edge onto the real line. Suppose $S$ is height $h = 3^{-n}$ above the real axis. Note that the (hyperbolic) length of $S$ is close to 2 if $A$ is large enough (it's length is $2 + O(e^{-A})$). Then $S$ hits the top edge of $m \in \{2, 3, 4\}$ ternary Carleson squares of Euclidean side length $h$.

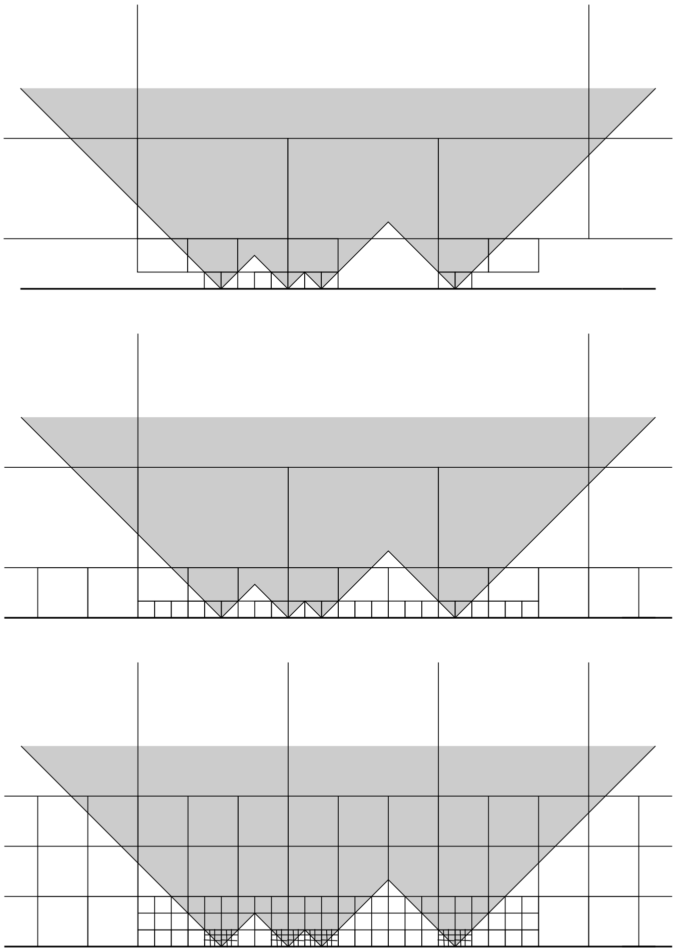

FIGURE 3. Cover the thick partof the sawtooth domain by Whitney boxes, cover the remainder by Carleson squares, cut the Whitney boxes into squares.

Denote the union these squares $R$. See Figure 4. Consider the square $Q$ among these that is farthest to the right. The right hand endpoint of $S$ is on the top edge of $Q$ and since segment of $\partial W$ passing though this point has slope 1, we see that the ternary Carleson sub-square of $Q$ of side length $h/3$ which is adjacent to $Q$'s right edge must miss $W$. Thus the top of this sub-square was not in $\mathcal{C}_1$ and so the sub-square is in $\mathcal{C}_1$. Similarly for the leftmost square hitting $S$. This means that if $R$ denotes the union of the ternary Carleson squares of side length $h$ hitting $S$, then every element of $\mathcal{C}_2$ hitting $\partial R \cap \mathbb{H}$ has the same side length, $h \cdot 3^{-k}$.

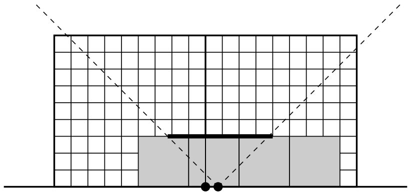

FIGURE 4. The collar squares at the bottom of a thin part. The rectangle $R$ is shaded and the "almost centered" Carleson squares are white.

Choose two disjoint and adjacent Carleson squares, $Q_1, Q_2$ of side length $3h$ so that so that $y = \partial Q_1 \partial Q_2 \cap \mathbb{R}$ is within $\frac{1}{2} \cdot 3^{-k}h$ of $x$, and $y$ is an integer multiple of $3^{-k}h$. Then the region $(Q_1 \cup Q_2) \setminus R$ can be divided into $2 \cdot 3^{2+k} - m \cdot 3^{2k}$ squares of side length $3^{-k}h$ and we add these squares to our collection. Note that each new square we just added which is adjacent to $R$ is the same size as the square in $\mathcal{C}_2$ that it touches.

Now suppose $S$ is the top edge of a thin part. Because the hyperbolic length of $S$ is close to 2 it can hit the bottom edge of either one or two Whitney boxes in $\mathcal{C}_1$. See Figure 5. Let $R$ be the union of all (either three or six) ternary Carleson squares of side length $h$ which lie under these squares. Choose two disjoint, adjacent Carleson squares of side length $h/3$ so that $y = \partial Q_1 \cap \partial Q_2 \cap \mathbb{R}$ is an integer multiple of $h \cdot 3^{-k}$ and is within $\frac{1}{2}h \cdot 3^{-k}$ of the point $x$ (as before this is the projection of the associated medial axis edge onto the real axis). Then the region $R \setminus (Q_1 \cup Q_2)$ can be tiled by squares of side length $h \cdot 3^{-k}$.

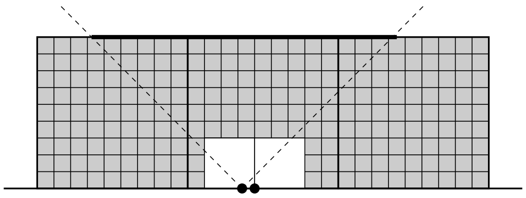

FIGURE 5. In each picture the rectangle $R$ is shaded and the "centered" Carleson squares are white. Top picture shows the construction at top edges of thin parts and the bottom picture corresponds

Add these "collar" squares to $\mathcal{C}_2$ to get a larger collection $\mathcal{C}_3$ and call their union $W_3$. Note that $W_3$ is a region in the upper half-plane that is tiled by Euclidean squares, each with a side length a power of 3 and that adjacent squares have side lengths differing by at most a factor of 3. Moreover, if $Q$ is a square, $\lambda > 0$ and $\lambda Q$ denotes the concentric square with side length $\lambda$ times that of $Q$, then for every $Q \in \mathcal{C}_3$, $3^k Q \cap S = \emptyset$, i.e., every square can be expanded by a factor of $M = 3^k$ and still miss $S$.

We can easily convert $\mathcal{C}_3$ to a quadrilateral mesh by subdividing squares if necessary. If a square shares edges with only four other squares we do nothing. Otherwise, it has one, two, three or four sides that subdivide into three edges each. The corresponding subdivision of the interior of the square is shown in Figure 6. Note that each of the quadrilaterals used has all angles between 45° and 135°.

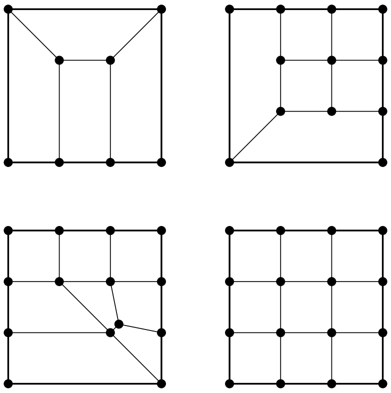

FIGURE 6. Subdividing a Whitney square into a quadrilateral mesh with angles between 45 and 135 so that no new vertices are added along the boundary.

In the next section we will transfer this mesh to a general polygon via a conformal map.

## 3. THICK AND THIN PARTS OF A POLYGON

In this section we use the conformal map from $\mathbb{H}$ to the interior of a polygon to define the thick and thin parts of the polygon. Strictly speaking, this definition is not needed for the proof of Theorem 1.1; the proof will continue in the next section. However, this decomposition is one of the motivations for the proof and I hope that by describing it, the proof will be a little easier to follow. Moreover, there are many interesting questions about the thick/thin decomposition and also many parallels with the theory of Riemann surfaces which may be useful in resolving other problems.

Let $\Omega$ be a simply connected plane domain whose boundary is an $n$-gon and let $f : \mathbb{H} \to \Omega$ is a a conformal map (we shall assume it preserves orientation and hence is 1-1 and holomorphic, i.e., a Riemann mapping). Since $\partial\Omega$ is locally connected, $f$ has a continuous extension to the $\partial\mathbb{H} = \mathbb{R} \cup \{\infty\}$ and there are $n$ points (called the prevertices) on $\partial\mathbb{H}$ which $f$ maps to the $n$ vertices of $\partial\Omega$. Without loss of generality we may assume three of these are $0, 1, \infty$ and that the others are all in $(0, 1)$. Let $S$ be the set of finite prevertices and let $W$ be the corresponding sawtooth region. Assume the notation of the previous section. We call $f(W^{\text{thick}})$ the thick part of $\Omega$ and it's complementary components in $\Omega$ the thin parts (more precisely, the $\epsilon$-thick and $\epsilon$-thin parts).

Actually, it would be better to say this is "a" thick/thin decomposition of $\Omega$, since the exact placement of the boundaries between the thick and thin pieces is arbitrary and it may be more convenient in other applications to define them differently (or even have the the thick and thin pieces overlap, as in [4]).

Although we have defined the thick and thin parts in terms of the conformal map from $\mathbb{H}$, it is possible to give a definition intrinsic to $\Omega$ which gives (roughly) the same decomposition. To describe this, we first need to recall the definition of extremal distance, a conformally invariant measure of the distance between two sets.

Suppose $\Gamma$ is a family of locally rectifiable paths in a planar domain $\Omega$ and $\rho$ is a non-negative Borel function on $\Omega$. We say $\rho$ is admissible for $\Gamma$ if

$$\ell(\Gamma) = \inf_{\gamma \in \Gamma} \int_\gamma \rho ds \geq 1,$$

and define the modulus of $\Gamma$ as

$$\mathrm{Mod}(\Gamma) = \inf_{\Omega} \int_M \rho^2 dxdy,$$

where the infimum is over all admissible $\rho$ for $\Gamma$. The reciprocal of the modulus is called the extremal length of the path family. These are important conformal invariants which are fundamental to the theory of conformal and quasiconformal mappings, and whose basic properties are discussed in many sources such as Ahlfors' book [1]. Basics examples to keep in mind include the path family connecting opposite sides of an $a \times b$ rectangle (if sides of length $a$ are connected the modulus is $a/b$) and the family connecting the inner and outer circles of a annulus (the modulus is $\log R/r$ if $R > r$ are the radii of the circles).

A generalized quadrilateral $Q$ is a Jordan domain in the plane with four specified boundary points $x_1, x_2, x_3, x_4$ (in counterclockwise order). We define the modulus of $Q$, $M_Q(x_1, x_2, x_3, x_4)$ (or just $M_Q$ or $M(Q)$ if the points are clear from context), as the modulus of the path family in $Q$ which connects the arc $(x_1, x_2)$ to the arc $(x_3, x_4)$. This is also the unique positive real number $M$ such that $Q$ can be conformally mapped to a $1 \times M$ rectangle with the arcs $(x_1, x_2)$, $(x_3, x_4)$ mapping to the opposite sides of length 1. We also call $1/\mathrm{Mod}(Q)$ the "extremal distance" from $(x_1, x_2)$ to the arc $(x_3, x_4)$ in $Q$. Roughly speaking, if the distance between two subarcs of $\partial Q$ is much smaller than the minimum of their diameters, then the extremal distance will be small.

Suppose $S \subset \mathbb{R}$ is a finite set and let $W$ be the corresponding sawtooth domain. We define a generalized quadrilateral by taking $Q = \mathbb{H}$ and the corners to be the endpoints of two components $I_1, I_2$ of $\mathbb{R} \setminus S$. Suppose $I_1$ is to the left of $I_2$ and let $J_1, J_2$ be edges of $\partial W$ over the right half of $I_1$ and the left half of $I_2$. Let $e$ be the edge of the medial axis of $W$ which bisects $J_1, J_2$, if such an edge exists and let $e$ be the empty set otherwise. If $I_1$ and $I_2$ share an endpoint then this is a degenerate quadrilateral and the extremal distance between $I_1$ and $I_2$ is 0. If the components are not adjacent, but $e$ is empty then one can show the extremal distance between $I_1$ and $I_2$ is bounded below uniformly. Otherwise, one can prove that

$$\mathrm{Mod}(Q) = \frac{1}{\pi \rho(e)} + O(1),$$

where $\rho(e)$ is the hyperbolic length of $e$. Thus we can identity the hyperbolic length of $e$, up to a constant additive factor, by the extremal distance of the corresponding intervals on $\mathbb{R}$. These intervals map to edges of $\partial\Omega$ and since extremal distance is a conformal invariant, we see that the thin parts of $\Omega$ are in 1-1 correspondence with pairs of edges on $\partial\Omega$ with small extremal distance in $\Omega$, and this is intrinsic to $\Omega$.

Computing the extremal distance between two sides of $\Omega$ exactly is difficult in practice, (probably as hard as computing the conformal map from $\Omega$ to $\mathbb{H}$ or $\mathbb{D}$) but for polygons the extremal distance can be estimated to within a multiplicative factor of $1 + \epsilon$ in time $O(n)$ (with constant depending on $\epsilon$) by results in [4]. Moreover, there is a relatively simple way to compute extremal distance up to a multiplicative factor of 8 given the medial axis of $\Omega$, using the so called "iota map", as described in [3]. Thus if we are only worried about the size of $\epsilon$ up to a fixed multiplicative factor, we can locate all the $\epsilon$-thin parts of a polygon in linear time using the medial axis (which itself can be computed in linear time).

The thick/thin decomposition of a polygon is motivated by a similar decomposition in the theory of hyperbolic manifolds (i.e., constant negative curvature), so I will say a few words about that case. If $M$ is a manifold and $x \in M$, the injectivity radius at $x$ is radius of the largest open ball around $x$ which is homeomorphic to a standard ball. Any larger ball contains a non-trivial loop through $x$ which cannot be deformed to a point. The $\epsilon$-thin parts of the manifold are the regions where the injectivity radius is $< \epsilon$. The remainder is called the thick part. See Figure **??**. It shows a hyperbolic surface (i.e., a Riemann surface) that has four thin parts. Three of these are cusps; they correspond to "punctures" in the surface which contain loops of arbitrarily small length as we approach the puncture. One thin part is hyperbolic; it is thin tube connecting two sections of the thick part and at the center is exponentially narrow as a function of its length.

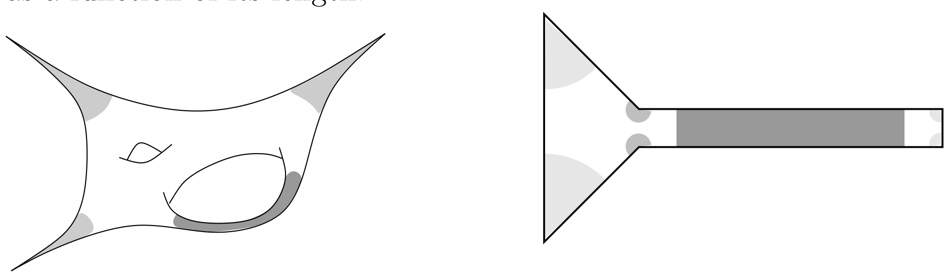

Figure 7. On the left is surface with a hyperbolic thin part (darker) and three parabolic thin parts (lighter). On the right is a polygon with one hyperbolic thin part (darker) and five parabolic thin parts.

A standard technique in the theory of hyperbolic manifolds is to partition the manifold into its thick and thin parts. Thin parts often cause technical difficulties, but this is partially compensated for by the fact that there are only a few possible types of thin parts and each has a well understood shape. Thus we can think of the manifold as consisting of some "interesting" thick parts attached to some annoying, but explicitly described, thin parts. The manifold is considered especially nice if no thin parts occur.

The thick/thin decomposition of polygons is analogous to that of surfaces. Indeed, one can form a surface by gluing two copies of the polygon along the interiors of it edges to form a surface homeomorphic to a sphere with $n$ punctures and the thin parts of this surface are in 1-1 correspondence with thin parts of the same type for the polygon (with comparable $\epsilon$'s).

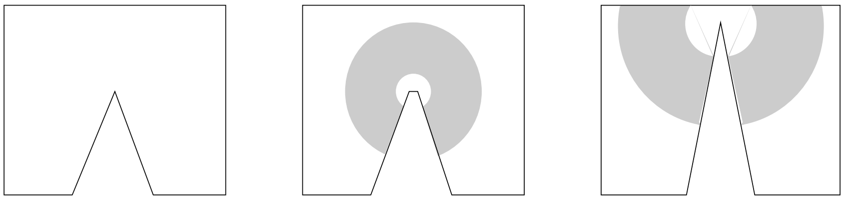

FIGURE 8. A thick polygon and two non-thick variations. The shaded areas correspond to hyperbolic thin parts.

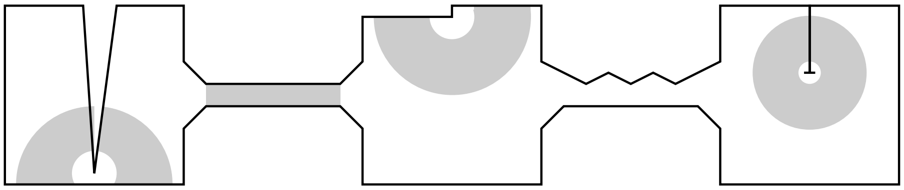

FIGURE 9. The five hyperbolic thin parts of this polygon are shaded gray.

We can always add more vertices to the boundary to make a polygon thick, although there is no bound on how many we might have to add. Also note that adding vertices can convert a thick polygon to a non-thick one, i.e., add two vertices $\epsilon$ apart to the middle of an edge of length 1.

## 4. Conformal mapping

We only need a few basic properties of conformal mappings. The first is Koebe's estimate (e.g. Cor. 4.4 of [9]): if $f$ is a conformal map between $\mathbb{D}$ and $\Omega$ then

$$\frac{1}{4}|f'(z)| \leq \frac{\operatorname{dist}(f(z), \partial\mathbb{D})}{\operatorname{dist}(f(z), \partial\Omega)} \leq 4|f'(z)|,$$

(and this is still true if $\mathbb{D}$ is replaced by any simply connected domain) and the closely related distortion theorem (Equation (4.17) of [9]).

$$\frac{1-|z|}{(1+|z|)^2} \leq \frac{|f'(z)|}{|f'(0)|} \leq \frac{1+|z|}{(1-|z|)^3},$$

The distortion theorem says that on small hyperbolic balls a conformal map is uniformly close to a linear map (since the derivative is close to a constant. By construction, $f$ is conformal on a large ball around each element of $\mathcal{C}_3$ (this is clear for pieces that were obtained as subsets of a Whitney box; for subsets of a Carleson square, the map $f$ can be extended to the reflection of the square across the real line by Schwartz reflection and this doubled squares contains a large ball around the piece). Thus $f$ is close to a conformal, linear map on each such quadrilateral and hence the image under $f$ of the vertices defines a quadrilateral in $\Omega$ that has almost the same angles and edge length ratios. Moreover, we can make them as close in shape to the originals as we want by simply making the elements of $\mathcal{C}_3$ small enough, i.e., by taking $M = 3^k$ large enough (but fixed independently of $n$ or $\Omega$). This gives the mesh on the thick part of the polygon.

In later sections we will show how to build the mesh on the thin parts by explicit constructions on each thin part. In order to merge these constructions with the mesh of the thick part given above, we will have to know that the conformal map has a certain behavior in the regions where the thick and thin parts meet (which is well inside a thin part with a larger value of $\epsilon$).

We claim that if the $\epsilon$ in the definition of thin part of $W$ is small enough then conformal map is close to a power function $z \to a + b(z-x)^\alpha$ on the thin part. Here, as before, $x$ is the vertical projection of the associated medial axis edge onto the real line. For parabolic thin parts this is easy since the thin part is mapped into a neighborhood of a vertex and this neighborhood looks like a cone near the vertex. The conformal map onto $\Omega$ can then be compared to the conformal map onto the cone (which is a power function) using the following result.

**Lemma 4.1.** *Suppose $A_\delta = \{z \in \mathbb{H} : \delta < |z| \leq \frac{1}{\delta}\}$ and suppose $Q$ is a quadrilateral with two opposite linear sides and two other sides which are either parallel line segments or circular arcs from concentric circles. Suppose $\Omega_1, \Omega_2$ are both simply connected domains which contain $Q$ and are obtained from $Q$ by replacing the second set of opposite edges by Jordan arcs. Suppose $f_1, f_2$ are conformal maps of $\mathbb{H}$ onto the simply connected domains $\Omega_1, \Omega_2$ and that $f_1(i) = f_2(i)$ and $\arg f_1'(i) = \arg f_2'(i)$. Then for $z \in A_{1/2}$ ,*

$$|f_1(z) - f_2(z)| \leq O(\delta|f'(i)|),$$

*and*

$$|f_1'(z) - f_2'(z)| \leq O(\delta|f'(i)|).$$

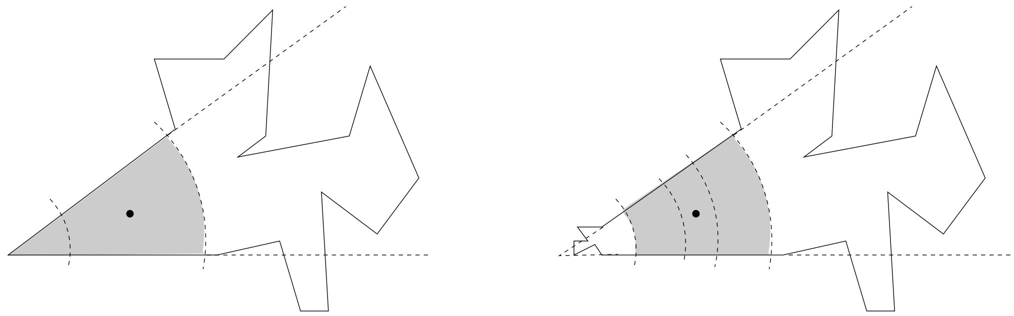

FIGURE 10. On the left is a parabolic thin part and on the right is a hyperbolic thin part . At points which are far (more than hyperbolic distance $A$) from the $\epsilon_0$-thick part the conformal map is close to a power function in the sense of Lemma 4.1.

In particular, since a power map sends lines through $x$ to lines through $f(x)$, the our map $f$ does almost the same thing in parabolic thin parts. Moreover, we still have the small angle distortion on small hyperbolic scales as described above. Suppose we have the situation illustrated in Figure 11; a polygonal curve which is the boundary of two equal sized Carleson squares with common corner $x \in \mathbb{R}$ and the arc of a circle with $y$ as its center and $|x - y| \le M/3$. Consider $4M$ even spaced points on this arc and project them radially onto the circle. It is a calculus exercise to check that the corresponding arcs on the circle all have angle measure within a factor of 2 of each other (the longest gaps are near the real line, the shortest correspond to the corners of the rectangular arc.

Then the radial lines map to curves that are almost radial in the sense that at each point they make an angle $\le \epsilon$ with the radius through the associated vertex. If $\epsilon$ is small with respect to $M$ then the straight lines connecting the images of the radial segments are disjoint. Moreover, by the distortion theorem the angle they make with the image segments from $\gamma_1$, $\gamma_2$ are close to the angles in $\mathbb{H}$. Since the original angles are between $45 - \epsilon$ and $90 + \epsilon$ we can take the angles in the images to be between $45 - 2\epsilon$ and $90 + 2\epsilon$.

The image of the circular arc, will not be an exact circular arc, but will be close to one and if we replace the image points by points on a true circular arc with spacing proportional to the spacing back in $\mathbb{H}$, the points will be moved so little that the change in angles is as small as we wish.

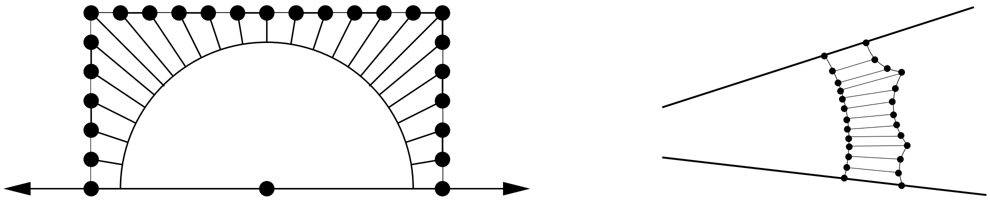

FIGURE 11.

The argument for hyperbolic thin parts is almost exactly the same, except that there is an additional approximation step that must be taken.

Define a collection $\mathcal{E}$ of elementary mapping functions, as all conformal maps of the upper half-plane to regions bounded by at most three straight edges (segments, rays or lines) with at most one bounded segment used. As special cases we take the functions $f(z) = az + b$ (one boundary line), $f(z) = az^\alpha + b$ (two boundary rays) and $f(z) = a \log z + b$ (two parallel boundary lines). When there are three sides there must be two rays and a finite segment.

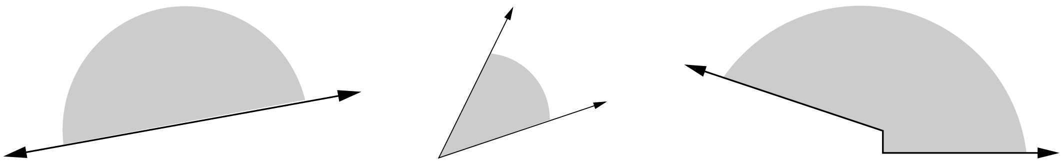

FIGURE 12. These are the special domains corresponding to $\mathcal{E}$.

The Schwarz-Christoffel formula gives a formula for the Riemann map of the upper half-plane onto a polygonal region $\Omega$: if the interior angles of $P$ are $\alpha\pi = \{\alpha_1\pi, \dots, \alpha_n\pi\}$, then

$$f(z) = A + C \int \prod_{k=1}^{n-1} (w - z_k)^{\alpha_k - 1} dw.$$

See e.g., [7], [10], [13]. On the half-plane the formula is The formula was discovered independently by Christoffel in 1867 [6] and Schwarz in 1869 [11], [12]. For other references and a brief history see Section 1.2 of [7].

The only case without an explicit formula is when $\mathbb{H}$ maps onto a region with three sides, and one vertex at $\infty$. In this case, we can place the prevertices at $\infty$ and any two finite points we want, say $\pm\epsilon$ and the derivative of the conformal map is

$$f'(z) = (z - \epsilon)^{\alpha_1 - 1}(z + \epsilon)^{\alpha_2 - 1}$$

which for points with $|z| \geq 1$ satisfies

$$f'(z) = z^{\alpha_1+\alpha_2-2} + O(\epsilon/|z|^2).$$

In particular, $f$ is close to the power map onto the cone corresponding to $\epsilon = 0$, i.e., radial segments in $\{|z| > 1\}$ are mapped to curves that are almost radial, in the sense that the angle they make with radial lines is $O(\epsilon/|z|^2)$.

So for hyperbolic thin parts, the mapping must approximate a mapping onto an elementary region, and the mapping for the elementary region approximates a power function, in the sense that radial lines map close to radial lines. With this observation, the proof for joining the mesh of a hyperbolic thin part to the mesh of thick part proceeds exactly like the parabolic case and we leave it to the reader.

Thus to finish the proof of Theorem 1.1 all we have to do is to find a mesh corresponding to each thin part so that the mesh covers a region bounded by parts of $\partial\Omega$ and polygonal arcs inscribed in circular arcs in $\Omega$ such that the angle measure of the inscribed arcs is given and has the property that any two arcs have measure within a factor of 2 of each other. This will be done in the next two sections.

The argument so far will only provide an existence proof of the desired quadrilateral mesh, since it involves evaluating the Riemann map between the polygonal domain $\Omega$ and the upper half-plane. However, all the required evaluations can be done with sufficiently small error in linear time, as given by the following version of the Riemann mapping theorem.

**Theorem 4.2.** *Suppose we are given a simply connected region $\Omega$ bounded by an $n$-gon and any $\epsilon > 0$. Then in time $O(n)$ (constant depending on $\epsilon$) we can compute a set $S \subset \mathbb{R}$, the mesh $\mathcal{C}_3$ corresponding to $S$, and a map $g$ on vertices of the mesh which extends to a $(1+\epsilon)$-quasiconformal map of the disk to $\Omega$ taking the set $S$ to the vertices of $\partial\Omega$. In particular, for any quadrilateral $Q$ in the mesh, the images of the vertices define a quadrilateral in $\Omega$ whose angles differ by at most a multiplicative factor of $1 + O(\epsilon)$ from the corresponding angles of $Q$. The total work is $O(n)$ where the constant may depend on $\epsilon$, but is no worse than $O(\log \frac{1}{\epsilon} \log\log \frac{1}{\epsilon})$.*

## 5. Meshing the hyperbolic thin parts

The hyperbolic thin parts are easy to mesh. They are bounded by two straight edges of $\partial\Omega$ and two polygonal arcs which approximate centric circular arcs connecting these line segments and we simply connect corresponding points on these arcs by straight lines. It is clear that all the angles are close to $90°$ is the number of points is large (e.g., $M$ is large) and the length of the finite segments is small (i.e., the $\epsilon$ in the definition of thin part is small enough). See Figure 13.

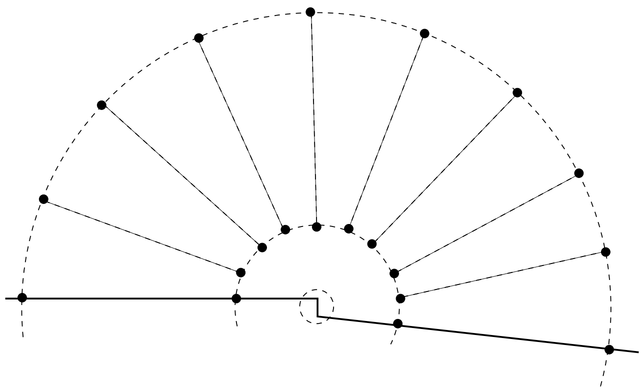

Figure 13. The mesh in a hyperbolic thin part is simply a bounded number of long, thin quadrilaterals whose sides approximate radial lines through a common point.

## 6. Meshing the parabolic thin parts

The parabolic thin parts correspond to neighborhoods of vertices of the polygon and will be meshed using an explicit set of quadrilaterals.

Associated to each vertex in $\partial\Omega$ will be a polygonal neighborhood (in $\Omega$) which has $2 + 4 \cdot 3^k$ sides. Two of these sides lie along the edges of $\partial\Omega$ which meet at the vertex. The other sides are inscribed on an arc $\gamma$ of a circle centered at the vertex and naturally correspond to subarcs of this arc. We will think of these subarcs as leaves of a rooted tree of intervals where the $\gamma$ is the root. It is divided into four equal length subarcs (it's children in the tree). Each of these is divided into three subarcs. The subarcs need not be equal length, but we will assume that any two arcs on the same generation have lengths differing by at most a factor of 2 (this will be used later in some estimates of angle sizes). We continue until we have all $4 \cdot 3^k$ children of $\gamma$.

This polygonal neighborhood of the vertex will be meshed by quadrilaterals with all new angles between $60^\circ$ and $120^\circ$. If $\Omega$ has angle $\le 120^\circ$ at $v$, then there is a quadrilateral of angle 120 with vertex at $v$ (so the angle is not subdivided). For large angles, more than one quadrilateral meet at $v$, but each has angle $\ge 60$ there.

Next we describe the mesh in each case.

**6.1.** $0 < \theta \le 120$**.** See Figure 14. The dashed lines are radial line segments through $v$ with define equal sized sectors (each of angle $\theta/4$) and the dashed arcs line on circles centered at $v$. The point $v$ is one vertex of a kite with opposite angle 120 (the other angles at this vertex are also 120) and in the center of the figure is a kite with a diagonal on the bisector of the angle at $v$ and angles $60, 90, 120, 90$ as shown. The other labeled angles satisfy

$$0 <\le \theta \le 120$$
$$60 \le \theta_1 = 120 - \frac{1}{2}\theta \le 120$$
$$60 \le \theta_2 = 90 - \frac{1}{4}\theta \le 90$$
$$75 \le \theta_3 = 90 - \frac{1}{8}\theta \le 90$$

$$60 \le \theta_4 = 360 - 120 - 2\theta_3 = 60 + \frac{1}{4}\theta \le 90$$
$$60 \le \theta_5 = 180 - 30 - \theta_2 = 60 + \frac{1}{4}\theta \le 90$$

$$60 \le \theta_6 = \theta_4 \le 90$$
$$60 \le \theta_7 = 360 - 120 - 90 - theta_6 = 150 - \theta_6 = 90 - \frac{1}{4}\theta \le 90$$
$$90 \le \theta_8 = 180 - \theta_4 = 120 - \frac{1}{4}\theta \le 120$$

**6.2.** $120 < \theta \le 240$**.** See Figure 15. As above the dashed lines define sectors of angle $\theta/4$ and the dashed arcs are concentric with $v$. In this case there are two quadrilaterals with $v$ as a vertex, each of angle $\theta/2$ which is between 60 and 90 degrees. These quadrilaterals are kites with opposite angle 120. The labeled angles

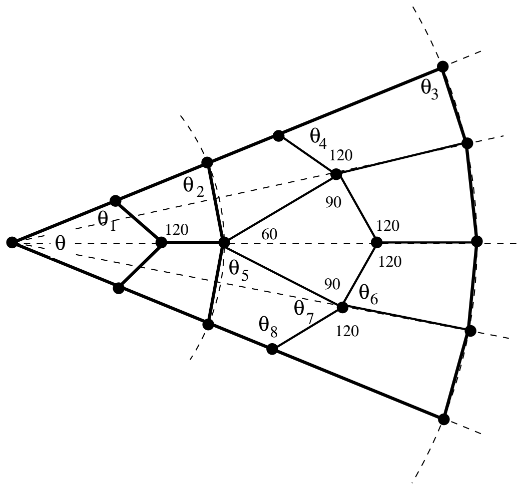


FIGURE 14.

satisfy

$$60 \le \theta_1 = 180 - 60 - \frac{1}{4}\theta = 120 - \frac{1}{4}\theta \le 90$$
$$60 \le \theta_2 = \frac{1}{2}(180 - \frac{1}{4}\theta) = 90 - \frac{1}{8}\theta \le 75$$

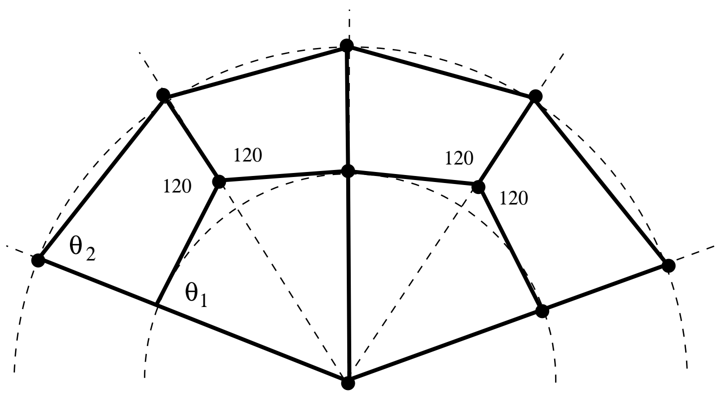


FIGURE 15.

6.3. $240 < \theta \le 360$**.** Divide each such angle into three equal angles. Each of these has measure between 80° and 120°. Apply the construction for angles between 0 and 120. This meshes a region near the angle which is bounded by 12 sides inscribed on a circular arc centered at the vertex.

6.4. **Splitting a section into three pieces.** See Figure 16. Note that new points are added along the edges and this requires that the same points be added to a splitter in an adjacent sector. Here we have

$$
\begin{aligned}
&0 <\leq \theta \leq 60\\
&60 \leq \theta_1 = 90 - \frac{1}{2}\theta \leq 90\\
&60 \leq \theta_2 = 360 - 60 - 2\theta_1 = 120 - \theta \leq 120\\
&60 \leq \theta_3 = 360 - 120 - 60 - \theta_1 = 90 - \frac{1}{2}\theta \leq 90
\end{aligned}
$$

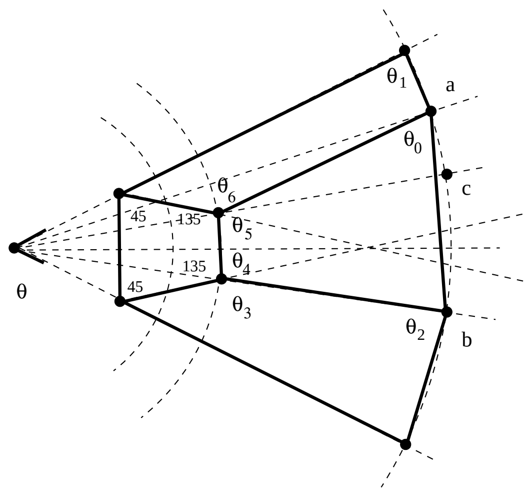


FIGURE 16.

How

## 7. Concluding remarks

What is the best $\theta$ for which every polygon can be meshed with quadrilaterals so that all new angles are between $\theta$ and $180 - \theta$? Can we take any $\theta = 60$?

The proof in this paper depends on a precise form of the Riemann mapping theorem which gives a linear bound on the work needed to approximate a conformal mapping to a polygon. In practice, this approximation may be too complicated to actually compute, but there are some ideas in the proof of the result which may be more directly related to meshing. I will describe two of these ideas here, but since they are easiest to understand for domains which are finite unions of disks, I will describe them in that setting (but they can be extended to polygons with some work, and perhaps to the class of circular arc polygons which contains both classes).

As is described in [4] any simply connected domain $\Omega$ which is a finite union of disks has a "normal crescent" decomposition as a finite union of crescents (a region bounded by two circular arcs) and ideal hyperbolic triangles (a region bounded by three pairwise tangent circle). The crescents have an obvious pair of orthogonal foliations: circular arcs through the pair of vertices and circular arcs perpendicular to the boundary arcs. These foliations can be continued into the gaps, except for a small triangle in the center of each gap. See Figure 17. Can we use these foliations to find a "nice" mesh of $\Omega$, e.g., one with quadrilaterals with angles close to $90°$ except near the vertices of the boundary and the triangles of the gaps?

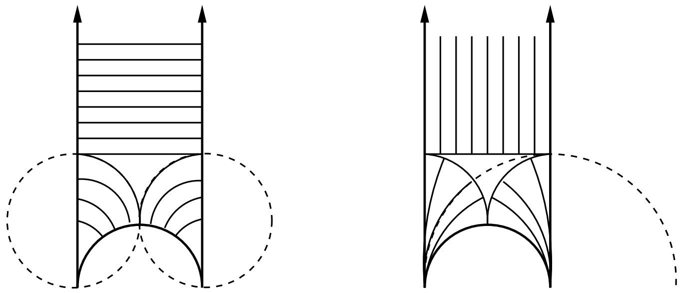

FIGURE 17. The $E$ and $G$ foliations of an ideal triangle (we have use a Möbius transformation to move the vertices to $0, 1, \infty$). Note that there is a central triangle which is not foliated.

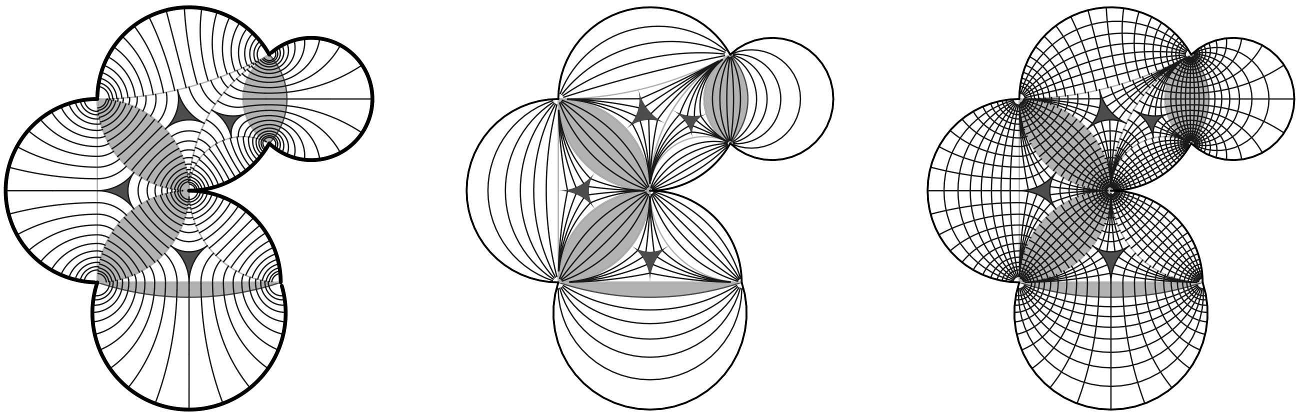

FIGURE 18. The $E$ and $G$ foliations for the finitely bent domain $\Omega_0$ (plotted separately and together)

The normal crescent decomposition is also useful because we can define a family of domains $\Omega_t$ by multiplying the angle of each crescent by a factor $t \in [0,1]$ and moving the gaps by appropriate Möbius transformations. When $t = 1$ we have the original domain. For $t = 0$ we get the disk (i.e., when we collapse the crescents to zero thickness, the gaps come together to form a disk). The important thing about this path of domains is that it is continuous in a quasiconformal sense, i.e., for $0 \leq s < t \leq 1$ there is an explicit quasiconformal map from $\Omega_s$ to $\Omega_t$ with QC-constant $O(|s-t|)$. This means that the map is close to conformal, i.e., perturbs angles by at most $O(|s-t|)$. Suppose that we have a problem that (1) we can solve for points on a circle and (2) given a solution for a domain we can find a solution on small quasiconformal perturbations. Then we can find a solution on $\Omega$ using $O(1)$ intermediate domains between $\mathbb{D}$ and $\Omega$. This is exactly the strategy used to prove the Riemann mapping theorem in [4]. Are there meshing problems that can be attacked in this way? A few examples of angle scaling families are given in Figures 19 to 20.

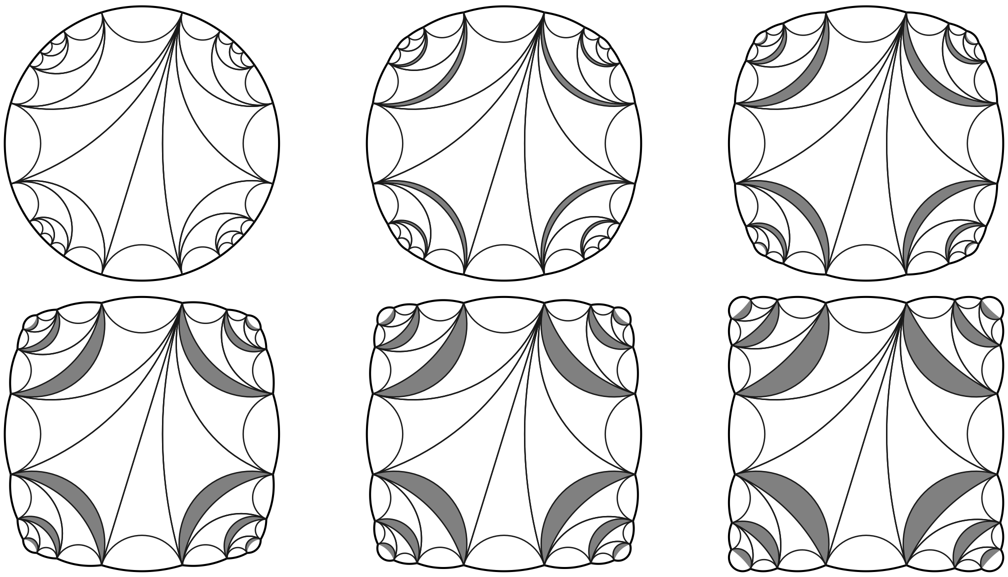

FIGURE 19. The one parameter family connecting the disk to an approximation of the square. In each picture the angles have been multiplied by $t = 0, .2, .4, .6, .8, 1$

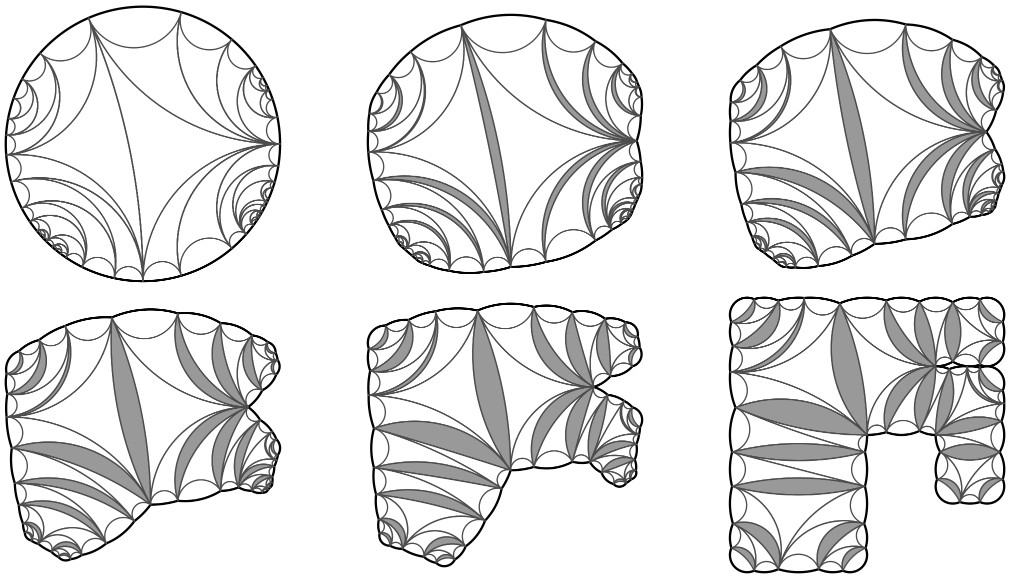

FIGURE 20.

## REFERENCES


[1] L. V. Ahlfors. *Lectures on quasiconformal mappings*. The Wadsworth & Brooks/Cole Mathematics Series. Wadsworth & Brooks/Cole Advanced Books & Software, Monterey, CA, 1987. With the assistance of Clifford J. Earle, Jr., Reprint of the 1966 original.

[2] M. Bern and D. Eppstein. Quadrilateral meshing by circle packing. *Internat. J. Comput. Geom. Appl.*, 10(4):347–360, 2000. Selected papers from the Sixth International Meshing Roundtable, Part II (Park City, UT, 1997).

[3] C.J. Bishop. A fast approximation to the Riemann map. 2003. Preprint.

[4] C.J. Bishop. Conformal mapping in linear time. 2006. Preprint.

[5] F. Chin, J. Snoeyink, and C. A. Wang. Finding the medial axis of a simple polygon in linear time. *Discrete Comput. Geom.*, 21(3):405–420, 1999.

[6] E.B. Christoffle. Sul problema della tempurature stazonaire e la rappresetazione di una data superficie. *Ann. Mat. Pura Appl. Serie II*, pages 89–103, 1867.

[7] T. A. Driscoll and L. N. Trefethen. *Schwarz-Christoffel mapping*, volume 8 of *Cambridge Monographs on Applied and Computational Mathematics*. Cambridge University Press, Cambridge, 2002.

[8] J. B. Garnett. *Bounded analytic functions*, volume 96 of *Pure and Applied Mathematics*. Academic Press Inc. [Harcourt Brace Jovanovich Publishers], New York, 1981.

[9] J.B. Garnett and D. Marshall. *Harmonic measure*. Cambridge University Press, Cambridge. to appear.

[10] Z. Nehari. *Conformal mapping*. Dover Publications Inc., New York, 1975. Reprinting of the 1952 edition.

[11] H.A. Schwarz. *Gesammelte Mathematische Abhandlungen*. Springer, Berlin, 1890.

[12] H.A. Schwarz. Confome abbildung der oberfläche eines tetraeders auf die oberfläche einer kugel. *J. Reine Ange. Math.*, pages 121–136, 1969. Also in collected works, [11], pp. 84-101.

[13] L. N. Trefethen and T. A. Driscoll. Schwarz-Christoffel mapping in the computer era. In *Proceedings of the International Congress of Mathematicians, Vol. III (Berlin, 1998)*, number Extra Vol. III, pages 533–542 (electronic), 1998.

C.J. Bishop, Mathematics Department, SUNY at Stony Brook, Stony Brook, NY 11794-3651
*E-mail address*: bishop@math.sunysb.edu